Proceedings of the XVIII ECSMGE 2024
GEOTECHNICAL ENGINEERING CHALLENGES
TO MEET CURRENT AND EMERGING NEEDS OF SOCIETY
© 2024 the Authors
ISBN 978-1-032-54816-6

ECSMGE 24
XVIII EUROPEAN CONFERENCE ON SOIL MECHANICS AND GEOTECHNICAL ENGINEERING

Class A predictions for centrifuge modelling of uplift induced instabilities of river embankments

Prévisions de classe A pour la modélisation en centrifugeuse des instabilités des berges induites par les pressions de soulèvement

E. Dodaro*, G. Gottardi
University of Bologna, Department of Civil, Chemical, Environmental and Materials Engineering, Bologna, Italy

M. Pirone, C. Mancuso
University of Napoli Federico II, Department of Civil, Building and Environmental Engineering, Napoli, Italy

R. Ventini
Ministry of Infrastructures and Transport, Interregional Public Works Department, Firenze, Italy

D. Giretti
University of Bergamo, Department of Engineering and Applied Science, 24044 Dalmine, Italy

C.G., Gragnano

Laboratoire Navier, Ecole des Ponts ParisTech, Gustave Eiffel University, CNRS, Marne-la-Vallée, France

V. Fioravante
University of Ferrara, Engineering Department, 44122 Ferrara, Italy

F. Zarattini, F. Gabrieli
University of Padova, Department of Civil, Environmental and Architectural Engineering, 35129 Padova, Italy

**elena.dodaro2@unibo.it (corresponding author)*

ABSTRACT: Flood events caused by the collapse of water-retaining earthworks are recognized as one of the most impactful natural disasters, affecting both urban and rural environment, as well as society and economy. The understanding of the peculiarities of different failure mechanisms is crucial for explaining the causes of breaching and assessing the safety of both new and existing earth infrastructures, under different hydraulic loading scenarios. This paper investigates the potential instability of the landside slope induced by high uplift pressures beneath the toe of a river embankment. This complex failure mechanism is largely influenced by the stratigraphy of the foundation soil and it might occur when embankment is constructed on alluvial plains with silty or clayey blankets overlying sandy soil strata, which act as preferential flow channel between the water basin and the landside. Results of a numerical predictive study carried out with the finite element method (FEM) on an unsaturated river embankment model, characterized by this peculiar subsoil layout, are presented and discussed. The impact of different thickness of the fine-grained layer on the potential failure mechanism has been evaluated, showing that this mainly affects the onset time of failure and the hydrometric level associated with its triggering. The analyses here presented provided fundamental insights for the design of a physical model test in a centrifuge.

RÉSUMÉ: Les inondations provoquées par l'effondrement des ouvrages de retenue d'eau sont parmi les catastrophes naturelles les plus dévastatrices, affectant tant les milieux urbains que ruraux, ainsi que la société et l'économie. Comprendre les divers mécanismes de défaillance est crucial pour expliquer les ruptures et évaluer la sûreté des infrastructures existantes et nouvelles, en tenant compte des conditions hydrauliques changeantes. Cet article se penche sur l'instabilité potentielle des talus terrestres, déclenchée par des pressions de soulèvement sous le pied d'une digue fluviale. Ce mécanisme complexe est largement influencé par la stratigraphie du sol de fondation et survient souvent lorsque la digue est érigée sur des plaines alluviales avec des couches limoneuses ou argileuses recouvrant des strates de sol sableux, servant de voies de circulation privilégiées entre le bassin hydrographique et le talus. Les résultats d'une étude numérique utilisant la méthode des éléments finis sur un modèle de digue non saturée sont présentés, fournissant des orientations essentielles pour la conception de tests en centrifugeuse. L'impact de différentes épaisseurs de la couche de grains fins sur le mécanisme de défaillance est évalué, démontrant que l'épaisseur influe principalement sur le moment et le niveau de déclenchement de la défaillance. Ces analyses constituent une base cruciale pour la conception de tests en centrifugeuse afin d'étudier les phénomènes physiques à petite échelle.

Keywords: River embankments; FEM numerical modelling; uplift pressure.

1 INTRODUCTION

Due to its profound impacts on the population, communication infrastructures, and economic and productive fabric, hydrogeological instability associated with the collapse of water-retaining earth structures constitutes a relevant issue for European countries. Therefore, identifying the main factors that adversely affect river embankment stability and trigger failure conditions is of particular concern for researchers and geotechnical engineers and represents a fundamental step for the optimal design and assessment of this critical infrastructure.

River embankment failure, defined as the inability to prevent the inundation of the area surrounding a watercourse, may occur due to various hydraulic and structural causes, such as overtopping, seepage flow through the embankment body and foundation layers, internal and external erosion, macro-instabilities of the slopes, scour and liquefaction (TAW, 1998; Van et al., 2022). Among macro-instabilities, it is possible to distinguish two mechanisms induced by the development of uplift pressures underneath the toe of the embankment that might lead to collapse: *(i)* backward erosion piping, involving the erosion and transportation of sand particles from the aquifer underlying a water-retaining structure, driven by underseepage forces; *(ii)* instability of the external slope of the embankment, due to a localized reduction in soil shear strength within the foundation.

This paper focuses on the second mechanism, which might occur when the subsoil is characterized by a shallow soft fine-grained layer, overlying a highly permeable sandy one, directly connected with the river and acting as a preferential channel between the reservoir and landside. In particular, if the water level increases, high pore water pressures can build up at the interface between the fine-grained and sandy layers, exceeding the overburden stress of the blanket on the landside. This circumstance may result in localized toe uplift and, simultaneously, favour the progression of a slip surface in the embankment body, resulting in a potential collapse, as evidenced in ICOLD (2013).

Despite the increasing occurrences of river embankment failures, there is a shortage of well-documented case studies of embankment collapse triggered by pore pressure build-up at the toe, with the exception of notable investigations carried out on some specific events. These include the embankment failure at Dartfort Lock (UK) in 1953, attributed by Cooling and Marsland (1961) to fine fissuring, as consequence of the abnormally high tides, which caused the development of high pore-water pressure in the underlying permeable sandy gravel layer. In the same year, a flood embankment collapsed at Crayford Marshes, on the south side of the River Thames, due to excessive pressures beneath the stratum of peaty clay alluvium, leading to slope instability of the outward face. In the Netherlands, the collapses of Wolpherense and Streefkerk river embankments in 1981 and 1984, respectively, have been also attributed to uplift pressures (Van et al., 2005), as well as the instability of a segment of the Adige river embankment near to San Floriano (Italy) in 1981, as reported by Amabile et al. (2020). In 2013 an embankment failure near Breitenhagen (Germany), was triggered by a localized weakness of the soil and to unexpected high water pressures, due a connection between a pond on the riverside of the earth structure and the aquifer (Kool et al., 2020).

To shed light on this complex failure mechanism, fully coupled flow-deformation analyses have been carried out using the software PLAXIS 2D (2021), on a river embankment model, subjected to a simulated river stage increment. The earthwork is characterized by an unsaturated silty sand embankment, supported by a fine-grained foundation overlying a sandy aquifer. Parametric analyses have been conducted by varying the thickness of the clayey silt foundation layer to explore its influence on the onset time of failure and to predict the critical hydraulic head, able to trigger the embankment failure.

The results of the simulations are presented and discussed hereafter. These findings provided crucial insights for the design of a centrifuge model test, executed at the Istituto Sperimentale Modelli Geotecnici - ISMGEO (Bergamo, Italy). To this aim, numerical simulations have been performed by considering the reduced physical model dimensions, to replicate the stress states expected during all the stages of the experiment. Further seepage and stability analyses were carried out at the prototype scale using various software on the same river embankment model and the outcomes of these studies are detailed in Girardi et al. (2022).

2 NUMERICAL MODELLING

2.1 Geometry and materials

The geometry of the river embankment numerically analysed is shown in Fig. 1, along with control points for displacements. It refers to a small-scale physical model. In centrifuge modelling the geometrical similitude (Taylor, 1995) is expressed by Eq. (1):

$$L_m/L_p = 1/N \quad (1)$$

where N is the scale factor for acceleration (i.e. $a_m = N\ a_p$), L_m and L_p are characteristic lengths of model and prototype, respectively. In the present case the model acceleration, a_m, has been assumed equal to 50 times the gravity. The embankment body is characterized by a height of 150 mm, a 60 mm wide crown and slopes inclination of 1H:1V and 1H:1.5V for the riverside and the landside, respectively (Fig. 1). The model has been numerically discretized with 4864 fifteen-triangular elements, with an average element size of 0.01 m. The foundation consists of a clayey silt deposit underlying a sandy layer, which extends beyond the landside toe and is hydraulically connected to the water basin on the riverside.

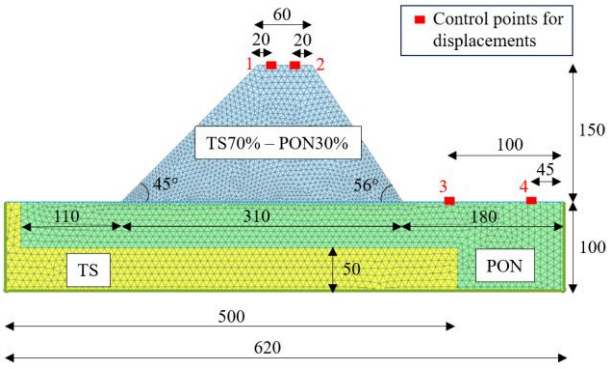

***Figure 1** - Geometry of the embankment section numerically analysed (in the case of 2.5 m-thick PON layer) in PLAXIS 2D - length unit at the model scale (in mm).*

The filling material selected for the embankment body, typically constituted by a heterogeneous mix of sands and silts, is a compacted mixture of 70% by weight of Ticino Sand (TS, a uniform, coarse to medium, clean sand) and 30% of Pontida Clay (PON, a sandy clayey silt), while for the upper layer of the subsoil, which frequently consists of clayey and silty strata, deposited in a floodplain environment, a homogeneous consolidated layer of PON is considered. For the aquifer a compacted TS layer has been adopted. The main index and physical properties of the three materials can be found in Fioravante and Giretti (2016) and Ventini et al. (2021). The optimum moisture content (w = 8.8%) and dry density (γ_d = 20.60 kN/m^3), determined using the Standard Proctor compaction energy, are taken as reference for the initial state (at 1g, i.e. before centrifuge acceleration) of the TS70% - PON30% mixture, while a pre-overburden vertical effective stress of 800 kPa has been considered for the PON layer. A relative density equal to 80%, with a water content of 5%, has been assumed to define the initial conditions of the TS layer.

2.2 Mechanical and hydraulic soil properties

The mechanical behaviour of the materials is modelled with the hardening soil (HS) constitutive model, developed by Duncan and Chang (1970) under the framework of the plasticity theory. Soil strength and stiffness parameters, calibrated based on specific laboratory procedures - extensively discussed in Ventini et al., (2021) - and assumed as input in the finite element analyses, are listed in Table 1.

***Table 1** - Mechanical properties of the embankment and foundation units, according to HS constitutive models.*

Soil		TS	TS70%-PON30%	PON
e	-	0.644	0.314	0.440
k_{sat}	m/s	$3.45\cdot10^{-5}$	$1.23\cdot10^{-7}$	$4.34\cdot10^{-9}$
γ_{dry}	kN/m^3	15.89	20.36	18.85
γ_{sat}	kN/m^3	20.00	22.30	21.09
ν	-	0.256	0.233	0.200
c'	kPa	0.1	5.0	4.0
φ'	°	41	46	33
$E_{50,\ ref}$	kPa	19800	22000	6000
$E_{oed,\ ref}$	kPa	14143	15000	4500
$E_{ur\ ref}$	kPa	59400	60000	20000
m	-	0.5	0.5	1.0
$K_{0,NC}$	-	0.344	0.287	0.455
OCR	-	1.0	1.0	6.9
POP	kPa	0	0	800

Hydraulic and retention properties of the mixture and PON, accurately estimated from constant head permeability tests, evaporation tests and high-range psychrometric measurements (Dodaro et al. 2024) are listed in Table 2, together with the saturated hydraulic conductivity of TS. The non-hysteretic Mualem-van Genuchten model (1980) was adopted for the fitting of the experimental data, through the parameters g_n, g_a, g_l. It is noted that the constitutive model adopted is able to take into account the influence of suction on soil shear strength, nevertheless, the dependence of compression index, C_c, on suction and the phenomena of wetting collapse, that distinguish the behaviour of unsaturated soils, are neglected.

***Table 2** - Hydraulic and retention parameters considered for the fully coupled flow-deformation analyses.*

Unit	k_{sat} (m/s)	S_{res} (-)	S_{sat} (-)	g_n (-)	g_a (1/m)	g_l (-)
TS 70% - PON 30%	$1.23\cdot10^{-7}$	0.057	1.000	1.240	0.821	-3.350
PON	$4.34\cdot10^{-9}$	0.000	1.000	1.455	0.070	-0.584
TS	$3{,}45\cdot10^{-5}$	-	-	-	-	-

2.3 Initial, boundary conditions and calculation stages

Imposing realistic initial conditions in terms of pore water pressure distributions is a crucial aspect when conducting transient seepage analyses of water-retaining earth structures. In the present numerical study, a uniform value of matric suction of about 5 kPa has been initially assigned to the embankment, to reproduce the physical model preparation state. In addition, an initial water head of 0.03 m (1.5 m at the prototype scale) has been applied for the time required to attain the equilibrium of pore water pressures in the whole model and to lead the aquifer to a saturated state (Fig. 4a). Regarding boundary conditions, since the model is expected to be contained in a rigid steel box, in the FE analysis, the bottom horizontal, right, and left vertical sides of the subsoil are assumed to be impermeable, with fully and horizontally fixed constraints, respectively. A zero head hydraulic conditions has been assigned to the top surface of the foundation on the landside, to simulate a water outlet zone. Furthermore, to model the interaction between the foundation soil and the container walls and to account for potential flow channels, three interface elements have been included. These last are characterized by a stiffness equal to the Young modulus of the steel and a hydraulic conductivity of 10^{-5} m/s. The progressive drying of the model due to evapo-transpiration phenomena has been neglected.

To replicate the centrifuge test plot, the following five calculation stages were considered: *I*) generation of initial stresses; *II*) construction of embankment; *III*) acceleration to the target; *IV*) self-weight equilibrium; *V*) river level rise. Details concerning each phase are reported hereafter and a scheme is provided in Fig. 2. Vertical and horizontal effective stress-fields have been initialized in *phase I* with the '*K0 procedure'* (PLAXIS 2D, 2021). To generate the preconsolidation stress state of the foundation strata at 1g, during the initial phase of the simulation, only the foundation layer has been activated and a pre-overburden pressure (POP) of 800 kPa has been imposed. During *phase II*, the 1g embankment construction has been simulated by means of an elastic-plastic deformation analysis ('*Plastic analysis' in* PLAXIS), in which the foundation is modelled as an undrained material, thus, excess pore water pressures have been calculated. The *'spin-up'* of the model, characterized by the gradual increase in the angular speed of centrifuge has been simulated through '*Consolidation analyses'*, by setting two different multiplier factors (*ΣM weight* equal to 24.3 and 50.6 g), uniformly applied on the whole numerical model, thus neglecting the distortion of the centrifugal field (*phase III*).

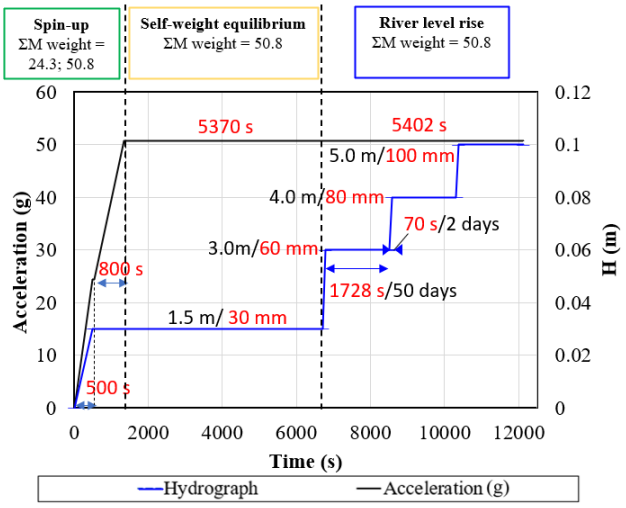

***Figure 2** - Time histories of the acceleration and water levels applied during the stages of the test (in red at the model scale and in black at the prototype scale) and calculation phases.*

Then, *'Fully coupled flow-deformation analyses'* have been carried out to simulate the dissipation of excess pore water pressure, resulting from the increase in the angular speed (*self-weight equilibrium stage, phase IV*) and to investigate the triggering of the failure mechanism caused by the rising of the water level (*flooding stage, phase V*) and the subsequent increase in the pore water pressure beneath the toe of the embankment. To identify the critical hydraulic head which would likely trigger a toe uplift mechanism, a time-dependent hydrometric condition, has been imposed on the riverside of the embankment (Fig. 2). Each water level was incrementally reached at a rate of about 14 mm/min and maintained for a period of 30 minutes, corresponding to about 50 days at the prototype scale, according to centrifuge scaling laws (Garnier et al., 2007), to guarantee the establishment of a steady-state flow regime within the embankment body at each step (Fig. 3).

The parametric study has been conducted by varying the fine-grained layer thickness, among 0.04 m, 0.05 m, and 0.06 m, while maintaining a constant dimension for the foundation (0.1 m). Consequently, the thickness of the sandy layer was adjusted accordingly.

3 RESULTS AND DISCUSSION

Fig. 3 shows FE numerical results, considering a 0.05 m-thick PON layer (2.5 m at the prototype scale) with reference to three significant time steps: a) at the beginning of the flooding stage (H = 0.03 m); b) at the end of the persistence of the first river stage; c) in correspondence of the triggering of the failure mechanism, occurred at H* = 0.073 m (3.65 m at the prototype scale). Following the first water level

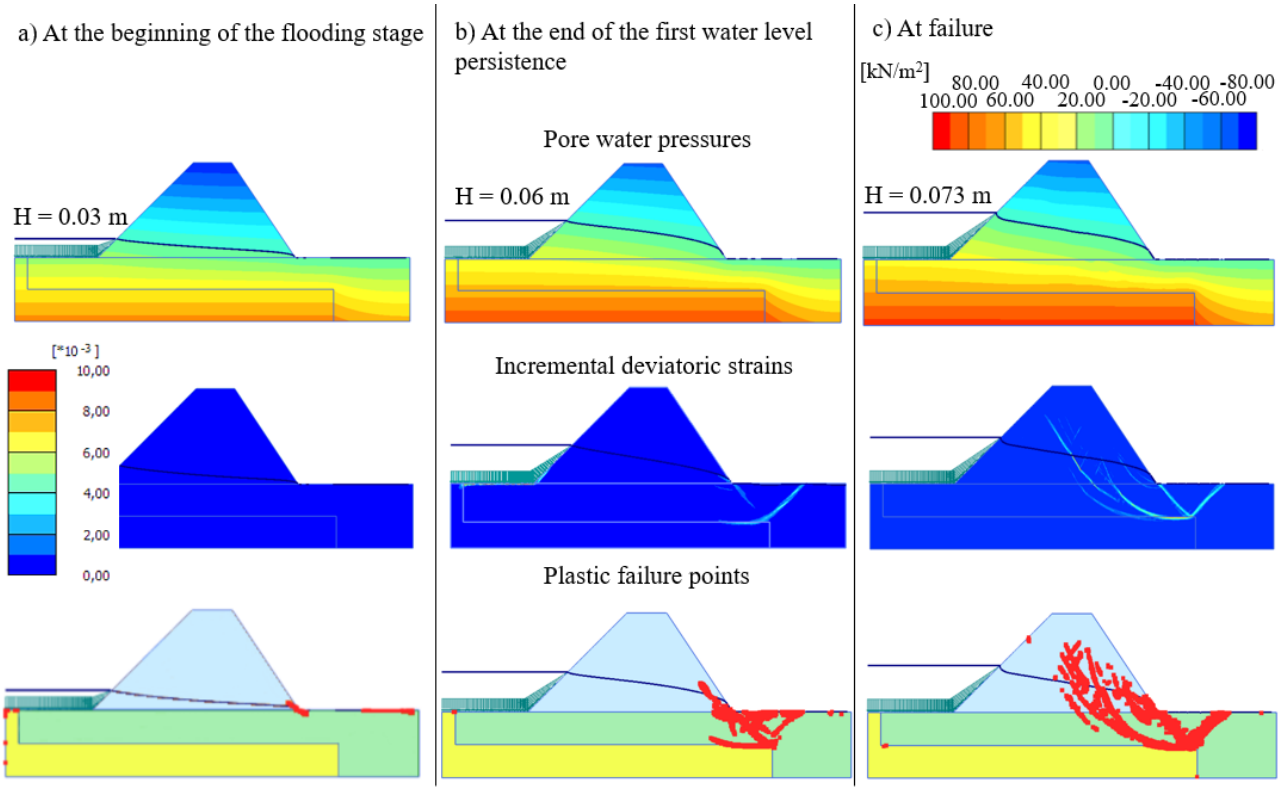

***Figure 3** - Pore pressures, total deviatoric strains and plastic failure points at different stages during FE analysis, considering a PON layer thickness of 0.05 m. Isoline increment = 10 kPa, phreatic surface in blue line.*

increment, a sudden increase of pore water pressures occurs in the aquifer. Then, the water level persistence leads to a progressive saturation of the lower part of the embankment body and, simultaneously, to a gradual rise in pore pressures, even in the fine-grained layer. The total deviatoric strains, initially extremely low and concentrated at the interface between PON and TS, gradually increase, as the phreatic surface advances within the earthfill. This progression is accompanied by a contextual decrease in vertical effective stresses in the PON layer, highlighting the shape of an instabile wedge and of potential slip surfaces within the embankment body, on the landside. Even the number of plastic failure points dramatically increase, as the hydrometric level rises to 0.073 m, suggesting a significant weakening of the embankment section, especially in correspondence of the landside toe, ultimately resulting in the collapse of the earth structure.

Fig. 4 reports the vertical displacement, u_y, calculated at the nodes highlighted in Fig. 1, throughout all stages of the analysis conducted with the 0.05 m-thick PON layer. During the centrifuge spin-up and the self-weight equilibrium stage, a gradual ground settlement associated with the consolidation of the PON layer was observed at nodes 1 and 2, located on the crest of the embankment. The settlement tendency diminished during the persistance of the first river stage, while at the critical head H*, displacements approached a vertical asymptote, evidencing the collapse of the embankment. After an initial settlement, during the second increment in water level, the ground surface on the landside began to ascend, with node 3 experiencing a higher rate of rise than node 4, indicating the occurrence of an uplift phenomenon near the toe of the embankment.

The correlation between the thickness of the PON layer and the critical hydrometric level for the three stratigraphy investigated is notably apparent in Fig. 5. In particular, the 0.04 m thick PON layer reaches a critical condition towards the end of the first water level persistence. Conversely, for thicknesses of 0.05 m and 0.06 m, the critical hydraulic heads, H*, are higher, i.e., 0.073 m (3.65 m at the prototype scale) and 0.08 m (4.0 m at the prototype scale), respectively. The foundation stratigraphy also influences the timing of failure onset. As the thickness of the PON layer increases, the time to reach conditions of potential instability also rises, as clearly highlighted by the trend depicted in red in Fig. 5. Pore pressures changes and deformations detected in the FE analyses, suggest an appropriate layout for the monitoring sensors. This layout should include tensiometers within the embankment body; pore pressure transducers in the foundation soils, concentrated at the interface between the the fine-grained and sandy layer, and displacement sensors positioned on the crest, the outward face and near the toe of the embankment.

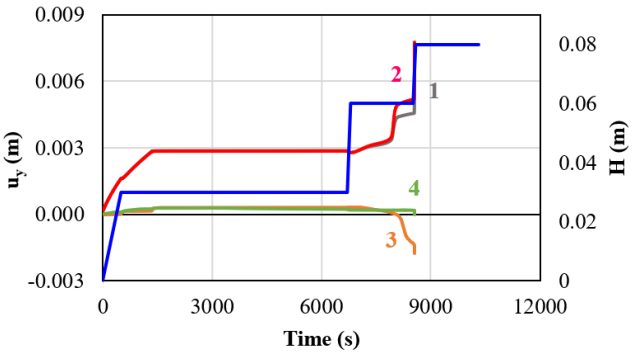

Figure 4 *- Vertical displacement calculated during the FE analysis on the crest of the embankment (1-2) and on the ground level on the landside (3-4). Settlements correspond to positive displacements.*

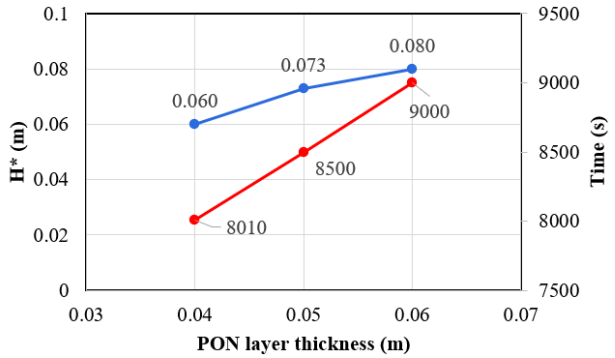

Figure 5 *– Effect of the PON thickness on the critical hydrometric level H* (in blue) and on the time of failure onset (in red).*

4 CONCLUSIONS

This paper presents and discusses the results of a numerical study carried out to investigate a failure mechanism for river embankments caused by uplift pressures beneath the toe. The main aim was to support the design of a centrifuge test. The study examines the influence of different foundation stratigraphy on the timing of failure and the hydrometric level associated to the collapse of the earthwork. In particular, as the thickness of the PON layer increases, the critical water level rises, and collapse occurs after a longer persistence of the flood event. Additionally, recommendations regarding an appropriate instrumentation layout for the centrifuge test were provided based on the outcomes of Finite Element Method (FEM) analyses.

ACKNOWLEDGEMENTS

The Authors would like to acknowledge the financial support from MIUR (Redreef – PRIN 2017, Grant agreement 2017YPMBWJ). We would also like to thank Prof. Claudio Mancuso, our friend and colleague and tireless PI of this project, who recently passed away.

REFERENCES

Amabile, A., Pozzato, A. and Tarantino, A. (2020) 'Instability of flood embankments due to pore-water pressure build-up at the toe: lesson learned from the Adige River case study', Canadian Geotechnical Journal, 57(12), pp. 1844–1853.

Bentley Systems Incorporated (2020) PLAXIS 2D-Reference Manual. Delft, The Netherlands.: Bentley Systems Incorporated.

Dodaro et al. (2024) 'Insights on the hydro-mechanical behaviour of a river embankment by physical and numerical modelling', Journal of Geotechnical and Geoenvironmental Engineering [Under review].

Duncan, J.M. and Chang, C.-Y. (1970) 'Nonlinear Analysis of Stress and Strain in Soils', Journal of the Soil Mechanics and Foundations Division, 96(5), pp. 1629–1653. https://doi.org/10.1061/JSFEAQ.0001458.

Fioravante, V. and Giretti, D. (2016) 'Unidirectional cyclic resistance of Ticino and Toyoura sands from centrifuge cone penetration tests', Acta Geotechnica, 11(4), pp. 953–968. https://doi.org/10.1007/s11440-015-0419-3.

Garnier, J. et al. (2007) 'Catalogue of scaling laws and similitude questions in geotechnical centrifuge modelling'. https://doi.org/10.13140/2.1.1615.3281.

Girardi, V. et al. (2023) 'Numerical Study of Uplift Induced Levee Failure for the Design of a Centrifuge Test', in C. Atalar and F. Çinicioğlu (eds.), 5th Int. Conf. on New Developments in Soil Mechanics and Geotechnical Engineering. Springer International Publishing pp. 213–221. https://doi.org/10.1007/978-3-031-20172-1_20.

ICOLD (2013) Internal Erosion of Existing Dams, Levees and Dykes, and Their Foundations. Bulletin 164, Vol. 1: Internal Erosion Processes and Engineering Assessment, International Commission on Large Dams, Paris.

Kool, J.J. et al. (2021) 'A Bayesian hindcasting method of levee failures applied to the Breitenhagen slope failure', Georisk: Assessment and Management of Risk for Engineered Systems and Geohazards, 15(4), pp. 299–316. https://doi.org/10.1080/17499518.2020.1815213.

TAW - Technical Advisory board Water barriers (1998) Foundation rules for water defence systems. Amsterdam: Balkema.

Taylor, R.N. (2018) 'Centrifuges in modelling: principles and scale effects', in R.N. Taylor (ed.) Geotechnical Centrifuge Technology. CRC Press, pp. 19–33.

Van Genuchten, M.T. (1980) 'A Closed-form Equation for Predicting the Hydraulic Conductivity of Unsaturated Soils', Soil Science Society of America Journal, 44(5), pp.892–898.

Van, M.A., Koelewijn, A.R. and Barends, F.B. (2005) 'Uplift Phenomenon: Model, Validation, and Design', International Journal of Geomechanics, 5(2), pp. 98–106.

Van, M.A., et al. (2022) Failure paths for levees. (ISSMGE) - Technical Committee TC201 'Geotechnical aspects of dikes and levees'. https://doi.org/10.53243/R0006

Ventini, R. et al. (2021) 'Experimental and Numerical Investigations of a River Embankment Model under Transient Seepage Conditions', Geosciences, 11(5), p. 192. https://doi.org/10.3390/geosciences11050192.